Studies of confinement: How quarks and gluons propagate

N. Brown and M. R. Pennington
Physics Department, Brookhaven National Laboratory, Upton, New York 11973
and University of Durham, Durham DH1 3LE, United Kingdom
(Received 24 March 1988)

Using the Schwinger-Dyson equations the behavior of quark and gluon propagators is studied in the Landau gauge for momenta from the deep Euclidean to the confinement regime. We find that while at short distances quarks and gluons propagate like free particles, over longer distances, of the order of a fermi, the gluon propagator is greatly enhanced as are the triple-gluon and quark-gluon couplings. These in turn suppress the propagation of massless quarks over long distances to such an extent that they have no physical particle pole, exactly as expected of a confining theory. We study the way the world changes as the number of massless flavors of quark is increased from zero. Even one generation of light fermions has a sizable deconfining effect on the one-gluon-exchange part of the interquark potential, greater than suggested by naive perturbative counting. These results highlight the usefulness of this continuum approach to nonperturbative QCD as a method of investigating the mechanics of confinement.

I. INTRODUCTION

When at high energies an electron and positron annihilate, they create for a tiny fraction of a second a quark and antiquark that jet apart. Many have modeled by Monte Carlo simulation how these separating partons emerge as hadrons at macroscopic distances.[1] But if QCD is the theory of strong interaction, it should be possible to calculate in terms of the fundamental parameters of the theory, its scale Λ and the masses of quarks, exactly how such a process proceeds. To achieve this we have to understand how to compute basic entities of the theory such as the propagators and couplings not just over short distances where perturbation theory can be successfully applied but over the longer distances of the size of hadrons, where a nonperturbative treatment is essential.

The Schwinger-Dyson equations provide a natural vehicle for such nonperturbative calculations,[2–7] being the field equations of the continuum theory. Unfortunately, the complete infinity of these nested integral equations is insoluble and simplifying assumptions are necessary to make any problem tractable. If we consider the pure gauge sector, as an illustration, the equation for the full two-point function involves the complete three- and four-point functions. These in turn satisfy equations which introduce the full five- and six-point functions explicitly. These in turn satisfy equations . . . *ad infinitum.* However, the beauty of a gauge theory lies in the way the Ward identities mean that the n-point function determines the $(n+1)$-point function, or at least that part of it that we may regard as longitudinal. This enables the Schwinger-Dyson equations to be truncated in a natural hierarchical fashion as Baker, Ball, and Zachariasen[4] have stressed. Then one can consistently model the behavior of the two-point functions, namely, the propagators, without the need to solve the infinity of equations. Although it is impossible formally to state how much one loses by such simplifications and truncations, the results are sufficiently realistic to make one believe they provide an adequate modeling of the small-scale universe inside the hadron interaction region—a step beyond perturbation theory.

Our aim here is to solve the coupled Schwinger-Dyson equations for the gluon and massless quark propagators. These are, of course, gauge-dependent entities and, for reasons advertised in Refs. 8 and 9, we choose to work in a covariant gauge (in the Landau gauge, in particular). To solve the coupled gluon and quark equations we adopt an iterative procedure. The strategy will be to solve the gluon equation in the absence of fermions, i.e., with $n_f=0$. This is the subject of Sec. II. Having found the behavior of the gluon propagator at essentially all relevant momenta, we feed this into the fermion equation, which forms the basis of Sec. III. We then determine the behavior of the fermion propagator for massless quarks and of the longitudinal part of the quark-gluon vertex. With these so specified we compute the contribution of quark loops to the gluon propagator. We show in Sec. IV that, as in the treatment in Ref. 10, their effect is far from negligible. We consequently introduce one flavor of quark into the gluon equation and solve this again. This solution is then substituted back into the fermion equation and thus resolved. Iterating a few times yields quark and gluon propagators that self-consistently satisfy the Schwinger-Dyson equations. The number of massless flavors is then increased to two and three in turn and the equations similarly solved. All this is detailed in Sec. IV. In Sec. V we discuss our results, which considerably extend those previously obtained in axial gauges,[4,7] and give our conclusions.

II. THE GLUON EQUATION

The aim of this section is to solve the Schwinger-Dyson equation for the gluon propagator in a world without quarks. This is largely a *necessary* recapitulation of the work of Refs. 5 and 8 with most of the details given in

Ref. 9. This gluon propagator is the foundation of all the calculations we subsequently discuss.

In Refs. 8 and 9, it has been shown that a satisfactory approximation to the Schwinger-Dyson equation for the gluon propagator, Fig. 1, is obtained by neglecting first all but the one-loop contributions, next by assuming the ghost contributions are essentially unrenormalized, and lastly by including only the longitudinal part of the full triple-gluon vertex, which is determined from the gluon propagator by the Slavnov-Taylor identity.[11,12] With the transverse part of the gluon propagator given by

$$\Delta_T^{\mu\nu}(p)=\frac{\mathcal{G}(p)}{p^2}\left[\delta^{\mu\nu}-\frac{p^\mu p^\nu}{p^2}\right] \tag{2.1}$$

the Schwinger-Dyson equation, Fig. 1, is an integral representation for the transverse part of its inverse

$$\Pi_T^{\mu\nu}(p)=\frac{1}{\mathcal{G}(p)}(p^2\delta^{\mu\nu}-p^\mu p^\nu) \tag{2.2}$$

being an identity for the longitudinal part. This equation (Fig. 1) for the gluon renormalization function $\mathcal{G}(p)$ has been solved in the Landau gauge in Refs. 8 and 9. Our truncation of the Schwinger-Dyson equations requires but a one-loop ultraviolet renormalization and this introduces just a single parameter: the QCD scale Λ. The solution shows $\mathcal{G}(p)$ to have a characteristically perturbative behavior for $p^2 \gg \Lambda^2$ and to increase as $1/p^2$ for $p^2 \ll \Lambda^2$, when all orders of perturbation theory are relevant, as expected of a confining theory.

However, a useful simplification of the equation of Fig. 1 has been proposed by Mandelstam.[5] As seen from Refs. 11 and 12, the longitudinal part of the full triple-gluon vertex always involves terms proportional to $1/\mathcal{G}$, with arguments p,k,k', where $k'=k-p$. There is obviously a partial cancellation of these with the $\mathcal{G}(k),\mathcal{G}(k')$ factors in the full propagators of Fig. 2(a). The approximation suggested by Mandelstam[5] is to assume this cancellation is complete and simply write the full vertex as $1/\mathcal{G}(k')$ times the bare triple-gluon vertex. This reduces the equation depicted in Fig. 1 to that in Fig. 3, where as in Ref. 8, we have neglected even the unrenormalized ghost contributions, noting their effect is *numerically* small. Projecting the equation, Fig. 3, with the tensor $P^{\mu\nu}=\delta^{\mu\nu}-4p^\mu p^\nu/p^2$ and performing the angular integrations gives simply

$$\frac{1}{\mathcal{G}(p)}=1+\frac{C_A g_0^2}{16\pi^2 p^2}\left[\int_0^{p^2} dk^2\mathcal{G}(k)\left[\frac{7k^4}{6p^4}-\frac{17k^2}{6p^2}-\frac{3}{8}\right]+\int_{p^2}^{\kappa^2} dk^2\mathcal{G}(k)\left[-\frac{7p^2}{3k^2}+\frac{7p^4}{24k^4}\right]\right], \tag{2.3}$$

where g_0 is the bare coupling, C_A the color factor for a gluon loop, viz., N_c, and κ is an ultraviolet cutoff introduced to render the integrals finite, which strictly determine $\mathcal{G}(p,\kappa)$. In Ref. 9 we have shown that this has all the structure of the more complete equation of Fig. 1, but in a far simpler form. Its solution for $\mathcal{G}(p)$ has the same qualitative behavior mentioned above for the equation with the full triple-gluon vertex and its more complex renormalization. Since these solutions have all the right features and Eq. (2.3) so much easier to solve computationally, we use it as the basis for our study of the behavior of both gluons and quarks we report here.

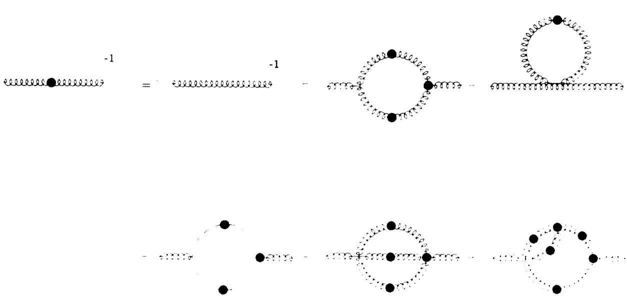

FIG. 1. The complete Schwinger-Dyson equation for the inverse gluon propagator with no fermions. The spiral lines represent gluons and the dashed lines ghosts. The dots denote full (as opposed to bare) propagators and vertices.

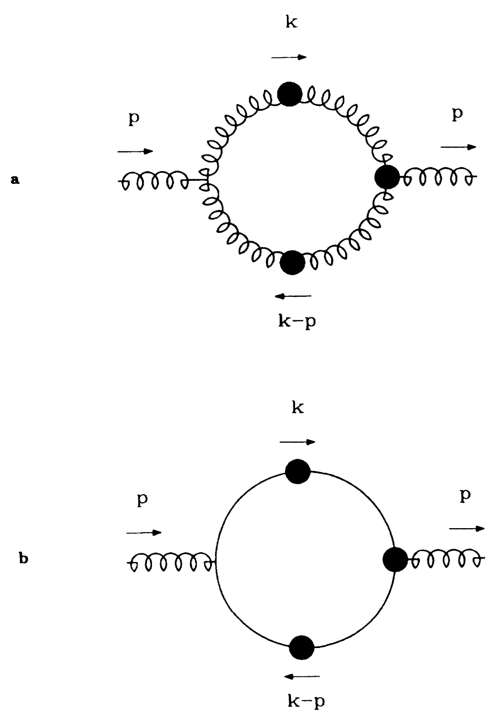

FIG. 2. (a) The one-loop gluon contribution to the inverse gluon propagator of Fig. 1 with the momenta labeled; (b) the one-loop quark contribution to the gluon propagator with the momenta labeled.

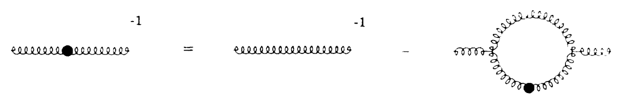

FIG. 3. Mandelstam approximation to the Schwinger-Dyson equation for the inverse gluon propagator (cf. Fig. 1).

Equation (2.3) is ultraviolet divergent in terms of the bare coupling g_0. Let us define a renormalized gluon function $\mathcal{G}_R(p)$ following the treatment of Ref. 4 by

$$Z_G(\kappa/\mu)\mathcal{G}_R(p)=\mathcal{G}(p,\kappa) \tag{2.4}$$

and a renormalized coupling $g(\mu)$ by

$$g^2(\mu)=Z_G(\kappa/\mu)^2 g_0^2 \ . \tag{2.5}$$

Using Eqs. (2.4) and (2.5) the running coupling, $\alpha_1(\mu)\equiv g^2(\mu)/4\pi$, satisfies

$$\alpha_1(p)=\alpha_1(\mu)\left[\frac{\mathcal{G}_R(p)}{\mathcal{G}_R(\mu)}\right]^2 \tag{2.6}$$

so that

$$\frac{1}{\mathcal{G}_R(p)}=\frac{1}{\mathcal{G}_R(\mu)}+\frac{C_A\alpha_1(\mu)}{4\pi}\int_0^\infty dk^2[\mathcal{J}(k,p)-\mathcal{J}(k,\mu)]\mathcal{G}_R(k) \ , \tag{2.7}$$

where the integral is now ultraviolet finite with the kernel $\mathcal{J}(k,p)$ being simply read off from Eq. (2.3). Although the coupling α_1 and the gluon renormalization function $\mathcal{G}_R$ are seemingly quite different from their analogs in Refs. 4, 8, and 9 with their more complete treatment of the triple-gluon vertex, their qualitative behavior is similar. The consistent renormalization of the Schwinger-Dyson equations is nontrivial and we shall distinguish the running coupling $\alpha_1(p)$ defined from the triple-gluon vertex from $\alpha_2(p)$, $\alpha_3(p)$ that are similarly related to the quark-gluon vertex used in Secs. III and IV (see Secs. IV and V for a comparison).

Expanding Eq. (2.7) in powers of $\alpha_1(\mu)$ we see that

$$\frac{1}{\mathcal{G}_R(p)}=\frac{1}{\mathcal{G}_R(\mu)}+\frac{\gamma_0'\alpha_1(\mu)}{4\pi}\ln\frac{p^2}{\mu^2} \ , \tag{2.8}$$

where $\gamma_0'=\frac{7}{3}C_A$ to be compared with the usual perturbative answer of $\gamma_0=\frac{13}{6}C_A$—the difference arising from our neglect of ghost loops. Similarly expanding Eq. (2.6) gives

$$\frac{1}{\alpha_1(p)}=\frac{1}{\alpha_1(\mu)}+\frac{\beta_0'}{4\pi}\ln\frac{p^2}{\mu^2} \ , \tag{2.9}$$

from which we see $\beta_0'=2\gamma_0'=\frac{14}{3}C_A$ (cf. $\beta_0=\frac{11}{3}C_A$ of usual perturbation theory). The standard renormalization-group improvement of the perturbative expansion of Eq. (2.8) gives asymptotically

$$\mathcal{G}_R(p)=\mathcal{G}_R(\mu)\left[\frac{\alpha_1(p)}{\alpha_1(\mu)}\right]^{\gamma_0'/\beta_0'} ; \tag{2.10}$$

here, $\gamma_0'/\beta_0'=\frac{1}{2}$.

Since it is not possible to find an analytic solution to Eq. (2.7) for subasymptotic momenta, we represent $\mathcal{G}_R(p)$ by a simple parametrization which reproduces this asymptotic form, Eq. (2.10), by introducing

$$\mathcal{G}_\infty(p)=\left[1+\frac{\beta_0'\alpha_1(\mu)}{4\pi}\ln\left[\frac{p^2}{\mu^2}+1\right]\right]^{-\gamma_0'/\beta_0'} . \tag{2.11}$$

We then input into the right-hand side of Eq. (2.7) the form

$$\mathcal{G}_R(p)=\frac{A\mu^2}{p^2}+\mathcal{G}_\infty(p)\left[\sum_{n=1}^{M}a_n\left[\frac{p^2}{p^2+p_n^2}\right]^{b_n}+\sum_{n=1}^{N}c_n\left[\frac{p^2\mu^2}{p^4+q_n^4}\right]^{d_n}\right] \tag{2.12}$$

allowing all of A, a_n, b_n, c_n, d_n, p_n, and q_n to vary. This is possible in the Mandelstam approximation as all the angular integrals have been explicitly evaluated in Eq. (2.3). This contrasts with the discussion of the gluon equation with the full triple-gluon vertex,[8,9] where both $\mathcal{G}(k)$ and $\mathcal{G}(k-p)$ appear. A similar situation will arise in the evaluation of the fermion equation (Sec. III), where the variation of the parametrization within the angular integrals has to be avoided because of the computing time required. As explained in Refs. 8 and 9, the appearance of the term $A\mu^2/p^2$ in the representation Eq. (2.12) does not prejudge that such an infrared singular behavior is required. The coefficient could turn out to be zero. However, as discussed in Refs. 3–6, 8, 9, and 13, this in fact does not happen for $n_f=0$, neither from numerical nor analytic investigations.

Setting $\mathcal{G}_R(\mu)=1$ with $\mu^2=10$ GeV^2, self-consistent solutions to Eq. (2.7) have been found for $0.01<p^2<40$ GeV^2 for a range of $\alpha_1(\mu)\in[0.15,0.3]$, i.e., $150<\Lambda<700$ MeV. The results, illustrating the input-output agreement, are shown in Fig. 4 for four values of $\alpha_1(\mu)$. The parameters of the solution with $\alpha_1(\mu)=0.25$ are listed in Table I as a typical example. These solutions form the basis for our calculations in Secs. III and IV. The momentum scale of the integral equations is wholly specified by μ and the value of the coupling $\alpha(p)$ at $p^2=\mu^2$.

III. THE FERMION EQUATION

The real world, of course, does not just contain gluons, but also the colored fermions "seen" in deep-inelastic scattering and in e^+e^- annihilation. Perturbatively, the effect of these quarks can be estimated from their contri-

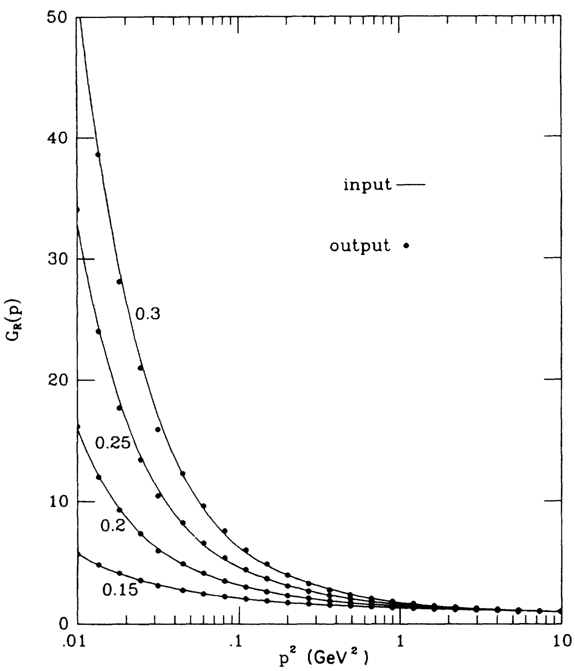

FIG. 4. Gluon renormalization function $\mathcal{G}_R(p)$ as a function of p^2 for four values of $\alpha_1(\mu)=0.15$, 0.2, 0.25, 0.3 with $n_f=0$.

bution to the one-loop β function:

$$\beta_0=\tfrac{11}{3}N_c-\tfrac{2}{3}n_f \;, \tag{3.1}$$

where N_c is the number of colors and n_f is the number of light-quark flavors. The naive counting given by this expression suggests that, perturbatively at least, the effect of even three flavors of light quarks will be small.

In a nonperturbative study, however, it is clear that we must calculate the dynamical effect of these fermions before we make any statements as to their relative importance compared to gluons. Writing the full fermion propagator for a massless quark as

$$S_F(p)=\frac{\mathcal{F}(p)}{\not p} \;, \tag{3.2}$$

it is the renormalization function $\mathcal{F}(p)$ that we wish to determine in analogy with $\mathcal{G}(p)$ for the gluon.

As a first step toward this, we examine the Schwinger-Dyson equation for the inverse fermion propagator, Eq. (3.3), which is shown diagrammatically in Fig. 5:

$$S_F^{-1}(p)=S_{0F}^{-1}(p) - \frac{g_0^2C_F}{16\pi^4}\int d^4k\,\gamma^\mu S_F(k')\Gamma^\nu(k',p)\Delta_{\mu\nu}(k) \;. \tag{3.3}$$

Here S_{0F} is the bare fermion propagator, i.e., Eq. (3.2) with $\mathcal{F}(p)\equiv 1$, g_0 is the bare coupling, C_F the appropriate color factor, viz., $(N_c^2-1)/2N_c$, and $\Gamma^\nu(k',p)$ is the full quark-gluon vertex.

Once we have included fermions in our theory, we must include their dynamical effect in the gluon equation through quark loops. As a first approximation, however, we can "quench" these contributions. We address the full equations in Sec. IV.

Since it is the infrared or low-momentum behavior we are particularly interested in, once again it is the longitudinal part of the vertex function which determines this.[12] It is now possible to use the Slavnov-Taylor identity for this quark-gluon vertex to determine its longitudinal part Γ_L^ν. Neglecting ghost contributions, this reduces to the Ward identity of an Abelian theory: namely,

$$q^\mu\Gamma_\mu^L(p,p')=S_F^{-1}(p)-S_F^{-1}(p') \;, \tag{3.4}$$

where q_μ is the incoming boson momentum. This can be solved[11] to give

$$\Gamma_\mu^L=\frac{1}{2}\gamma_\mu\left[\frac{1}{\mathcal{F}(p)}+\frac{1}{\mathcal{F}(p')}\right] + \frac{1}{2}(p+p')_\mu(\not p+\not p')\left[\frac{1}{\mathcal{F}(p)} - \frac{1}{\mathcal{F}(p')}\right]\frac{1}{p^2-p'^2} \;. \tag{3.5}$$

Using this, and our solution for the gluon function $\mathcal{G}(p)$ obtained in Sec. II, we now have a closed integral equation for the fermion renormalization function $\mathcal{F}(p)$:

$$\frac{\not p}{\mathcal{F}(p)}=\not p-\frac{g_0^2C_F}{16\pi^4}\int d^4k\frac{\gamma_\mu \not k'\Gamma_\nu^L}{k'^2k^4}(k^2\delta^{\mu\nu}-k^\mu k^\nu) \times\mathcal{G}(k)\mathcal{F}(k') \;. \tag{3.6}$$

Note here we are only concerned with the class of solutions to the fermion equation, Eq. (3.3), in which no

TABLE I. Parameters of the gluon function $\mathcal{G}_R(p)$ as specified in Eq. (2.12) for the solution with $\alpha_1(\mu)=0.25$ for $n_f=0,2,4,6$.

n_f	0	2	4	6
A	0.032 54	0.020 82	0.010 46	0.003 833
a_1	0.9744	0.9761	0.9467	0.9454
p_1 (GeV)	0.4501	0.4524	0.3935	0.4120
b_1	1.198	1.296	1.128	0.4215
c_1	0.1079	0.1155	0.1299	0.1054
q_1 (GeV)	0.3870	0.3250	0.2441	0.1695
d_1	0.6605	0.6194	0.5188	0.4620

FIG. 5. The complete Schwinger-Dyson equation for the inverse quark propagator. The solid lines represent quarks, the spiral lines gluons. The dots denote full (as opposed to bare) propagators and vertices.

dynamical mass is generated, which we believe is not unrealistic for the first generation of quarks. Formally such a solution always exists for vertex functions of the form of Eq. (3.5). The important question of chiral-symmetry breaking has been addressed in Refs. 14 in toy models and more realistically in Refs. 7, 15, and 16.

Returning to Eq. (3.6) we take its trace, having multiplied by $\not p$ to obtain

$$\frac{1}{\mathcal{F}(p)}=1-\frac{g_0^2C_F}{16\pi^4}\int d^4k\frac{\mathrm{Tr}(\not p\gamma_\mu \not k'\Gamma^L_\nu)}{4p^2k'^2k^4}\times(k^2\delta^{\mu\nu}-k^\mu k^\nu)\mathcal{G}(k)\mathcal{F}(k') \ . \tag{3.7}$$

Explicitly evaluating the trace and performing the Lorentz contraction gives

$$\frac{1}{\mathcal{F}(p)}=1-\frac{g_0^2C_F}{16\pi^4}\int d^4k\frac{\mathcal{G}(k)\mathcal{F}(k')}{p^2k'^2k^4}\left[I_1(k,p)\left[\frac{1}{\mathcal{F}(p)}+\frac{1}{\mathcal{F}(k')}\right]+I_2(k,p)\left[\frac{1}{\mathcal{F}(p)}-\frac{1}{\mathcal{F}(k')}\right]\frac{1}{p^2-k'^2}\right] , \tag{3.8}$$

where

$$\begin{aligned}I_1(k,p)&=\tfrac{3}{2}k^2k\cdot p-\tfrac{1}{2}p^2k^2-(k\cdot p)^2 \ ,\\ I_2(k,p)&=k^4p^2-k^2(k\cdot p)^2-2k^2p^2(k\cdot p)\\ &\quad+2(k\cdot p)^3-2p^2(k\cdot p)^2+2p^4k^2\\ &=(k^2+p^2)[k^2p^2-(k\cdot p)^2] \ .\end{aligned} \tag{3.9}$$

It is not possible to solve Eq. (3.8) analytically, and so we will choose a parametrization for $\mathcal{F}$ (much as for $\mathcal{G}$ in Sec. II) and attempt a numerical solution. Before we do this, however, it is necessary to investigate analytically what form our parametrization should take.

(i) If $\mathcal{F}(p)\sim\mu^2/p^2$ as $p^2\to 0$ then the left-hand side of Eq. (3.8) behaves as p^2/μ^2 in this limit. The behavior of the right-hand side of the equation is given by the form of $\mathcal{G}(k)$, which, from Sec. II, behaves like μ^2/p^2 as $p^2\to 0$. On dimensional grounds we get the same behavior for the right-hand side, and we see that consistency is not possible in this limit.

(ii) If $\mathcal{F}(p)\sim$const as $p^2\to 0$ then by a similar argument to (i) above, the left-hand side behaves like a constant, while the right-hand side behaves like μ^2/p^2. Again consistency is impossible.

(iii) If $\mathcal{F}(p)\sim p^2/\mu^2$ as $p^2\to 0$ then the left-hand side of the equation behaves like μ^2/p^2. The behavior of the right-hand side is the same as in (i) and (ii) above, and we see that consistency is possible.

The above analysis reveals that a consistent solution is permitted for $\mathcal{F}$ vanishing at small p^2, as Ball and Zachariasen have deduced in an axial gauge.[7] However, we have not yet proven that the fermion equation does indeed demand this behavior. In order to demonstrate that, we must numerically investigate Eq. (3.8) to see if such a solution is in fact allowed.

As for the gluon equation, let us cast Eq. (3.8) in the form

$$\frac{1}{\mathcal{F}(p)}=1-\frac{g_0^2C_F}{16\pi^4}\int d^4k\ \mathcal{G}(k)\mathcal{H}(k,p)-\frac{g_0^2C_2(F)}{16\pi^4}\frac{1}{\mathcal{F}(p)}\int d^4k\ \mathcal{G}(k)\mathcal{F}(k')\mathcal{L}(k,p) \ , \tag{3.10}$$

where

$$\begin{aligned}\mathcal{H}(k,p)&=\frac{1}{k^4k'^2p^2}[I_1(k,p)+k^2p^2-(k\cdot p)^2] \ ,\\ \mathcal{L}(k,p)&=\frac{1}{k^4k'^2p^2}\left[I_1(k,p)-k^2p^2+(k\cdot p)^2+2p^2\left[\frac{k^2p^2-(k\cdot p)^2}{k'^2+p^2}\right]\left[\frac{\mathcal{F}(p)}{\mathcal{F}(k')}-1\right]\right] .\end{aligned} \tag{3.11}$$

At this stage $\mathcal{F}(p)$ is formally $\mathcal{F}(p,\lambda,\kappa)$, where λ,κ are infrared and ultraviolet cutoffs, respectively, introduced to make the integrals in Eq. (3.10) finite. Infrared divergences only arise from the $1/k^2$ term in $\mathcal{G}(k)$ and only then in the second integral involving $\mathcal{L}(k,p)$, the other being infrared finite. To deal with the ultraviolet divergences we define a running coupling by

$$g^2(\mu)=\frac{g_0^2Z_G(\kappa/\mu)}{1-(g_0^2C_F/16\pi^4)\int d^4k\ \mathcal{H}(k,\mu)\mathcal{G}(k,\kappa)} \ , \tag{3.12}$$

where we introduce the renormalized functions $\mathcal{G}_R$ (as in Sec. II) and $\mathcal{F}_r$ specified by

$$Z_G(\kappa/\mu)\mathcal{G}_R(p)=\mathcal{G}(p,\kappa) \ , \tag{3.13}$$

$$Z_F(\kappa/\mu,\lambda/\mu)\mathcal{F}_r(p,\lambda)=\mathcal{F}(p,\lambda,\kappa) .$$

The definition of $g^2(\mu)$ in Eq. (3.12) involves infrared finite quantities and so this coupling is independent not only of κ, but also λ. By virtue of Eq. (3.10), Eq. (3.12) can be written

$$g^2(\mu)=\frac{g_0^2 Z_G(\kappa/\mu)Z_F(\kappa/\mu,\lambda/\mu)\mathcal{F}_r(\mu,\lambda)}{1+(g_0^2 C_F/16\pi^4)Z_F(\kappa/\mu,\lambda/\mu)\int d^4k\, \mathcal{L}(k,\mu)\mathcal{G}(k,\kappa)\mathcal{F}_r(k',\lambda)} . \tag{3.14}$$

Because of Eq. (3.12) the numerator and denominator of Eq. (3.14) must have canceling λ dependence. Equation (3.10) can now be written in terms of the coupling $\alpha_2(\mu)\equiv g^2(\mu)/4\pi$, which can be manipulated into the form

$$\frac{1}{\alpha_2(p)}=\frac{\mathcal{G}_R(\mu)}{\mathcal{G}_R(p)}\left[\frac{1}{\alpha_2(\mu)}-\frac{C_F}{4\pi^3}\int d^4k\, \mathcal{G}_R(k)[\mathcal{K}(k,p)-\mathcal{K}(k,\mu)]\right] . \tag{3.15}$$

For a discussion on the consistency of this definition of the coupling with that of the triple-gluon vertex $\alpha_1(\mu)$ introduced in Sec. II, see Sec. V. In the perturbative regime we can expand this in powers of $\alpha_2(\mu)$ giving

$$\frac{1}{\alpha_2(p)}=\frac{1}{\alpha_2(\mu)}+\frac{\beta_0''}{4\pi}\ln\frac{p^2}{\mu^2} , \tag{3.16}$$

where $\beta_0''=\frac{7}{3}C_A+\frac{3}{4}C_F$. Some algebraic rearranging allows us to write the ultraviolet renormalized equation as

$$\frac{\mathcal{F}_r(\mu,\lambda)}{\mathcal{F}_r(p,\lambda)}=1-\frac{\alpha_2(\mu)C_F}{4\pi^3}\left[\int d^4k\, \mathcal{G}_R(k)[\mathcal{K}(k,p)-\mathcal{K}(k,\mu)] .\right.$$
$$\left.+\frac{1}{\mathcal{F}_r(p,\lambda)}\int d^4k\, \mathcal{G}_R(k)[\mathcal{L}(k,p)\mathcal{F}_r(k',\lambda)-\mathcal{L}(k,\mu)\mathcal{F}_r(k'',\lambda)]\right] , \tag{3.17}$$

where $k''=k-\mu$.

So far we have performed essentially a one-loop ultraviolet renormalization. To discover the asymptotic form of $\mathcal{F}$, we can now expand $\mathcal{F}=1+O(\alpha_2)$. As in standard perturbation theory in the Landau gauge, $\mathcal{F}$ is finite to one loop. Thus to $O(\alpha_2)$,

$$\mathcal{F}\rightarrow\text{const} \tag{3.18}$$

asymptotically.

Before we can proceed further, we must deal with the infrared divergences which arise from the enhanced $A\mu^2/k^2$ term in the gluon propagator. Let us explicitly display the λ dependence of Eq. (3.17) by writing it as

$$\frac{\mathcal{F}_r(\mu,\lambda)}{\mathcal{F}_r(p,\lambda)}=1+A(p,\mu)+\frac{1}{\mathcal{F}_r(p,\lambda)}\left[B(p,\mu)+C(p,\mu)\ln\frac{\lambda}{\mu}\right] , \tag{3.19}$$

where A,B,C are determined by the integrals of $\mathcal{K},\mathcal{L}$ in Eq. (3.17). A is trivially infrared finite while B and C are linear in $\mathcal{F}_r$. Nevertheless, C has an explicitly derivable analytic expression independent of the form of $\mathcal{F}_r(p,\lambda)$. The λ dependence can now be eliminated by first evaluating Eq. (3.19) at $p^2=\mu'^2$ and substituting the value of $\mathcal{F}_r(\mu',\lambda)$ to give

$$\frac{1}{C(p,\mu)}\{\mathcal{F}_r(\mu,\lambda)-B(p,\mu)-\mathcal{F}_r(p,\lambda)[1+A(p,\mu)]\}=\frac{1}{C(\mu',\mu)}\{\mathcal{F}_r(\mu,\lambda)-B(\mu',\mu)-\mathcal{F}_r(\mu',\lambda)[1+A(\mu',\mu)]\} . \tag{3.20}$$

Since both the left- and right-hand sides of this equation are linear in $\mathcal{F}_r$, let us define a factor $Z_{\text{IR}}(\lambda/\mu)$ such that

$$Z_{\text{IR}}(\lambda/\mu)\mathcal{F}_r(p,\lambda)=\mathcal{F}_R(p) . \tag{3.21}$$

Multiplying Eq. (3.20) by Z_{IR}, all quantities are then well defined in the limit $\lambda\rightarrow 0$, so that

$$\frac{\mathcal{F}_R(\mu)}{\mathcal{F}_R(p)}=1+A(p,\mu)+\frac{B(p,\mu)}{\mathcal{F}_R(p)}+\frac{C(p,\mu)}{C(\mu',\mu)}\frac{1}{\mathcal{F}_R(p)}[\mathcal{F}_R(\mu)-\mathcal{F}_R(\mu')]-\frac{C(p,\mu)}{C(\mu',\mu)}\frac{\mathcal{F}_R(\mu')}{\mathcal{F}_R(p)}\left[A(\mu',\mu)+\frac{B(\mu',\mu)}{\mathcal{F}_R(\mu')}\right] . \tag{3.22}$$

In order for the $\ln\lambda$ terms to cancel, $\mathcal{F}_r(\mu',\lambda)$ must be the same function of μ' as $\mathcal{F}_r(p,\lambda)$ is of p. Unlike an ultraviolet renormalization where the value of $\mathcal{F}_R(\mu)$ is not determined, the nonlinearity of Eq. (3.22) specifies $\mathcal{F}_R(\mu')$. We can then solve Eq. (3.22) to determine $\mathcal{F}_R(p)$ completely. However, an easier way to proceed is to return to Eq. (3.20) with $\mathcal{F}_r(p,\lambda)$ now replaced by $\mathcal{F}_R(p)$. It is then clear that the left-hand side is a function of p independent of μ', and the right-hand side is a function of μ' independent of p, and hence each side is a constant, which can be written as $\ln\delta/\mu$. Thus $\mathcal{F}_R(p)$ satisfies

$$\frac{\mathcal{F}_R(\mu)}{\mathcal{F}_R(p)}=1+A(p,\mu)+\frac{1}{\mathcal{F}_F(p)}\left[B(p,\mu)+C(p,\mu)\ln\frac{\delta}{\mu}\right] \tag{3.23}$$

with δ a parameter determined by this equation, which is of course symbolically the same as Eq. (3.19), but now with all quantities independent of the arbitrary infrared cutoff, λ. That this is a correct procedure was explicitly shown by first solving Eq. (3.22) to find a solution $\mathcal{F}_R(p)$, and then determining the value of $\ln\delta$ from Eq. (3.23) for *all* values of p^2 for which we numerically solved the equation. For $0.01<p^2<100$ GeV^2, we found that $\ln\delta$ varied by only a few percent. Solving Eq. (3.23) directly with $\ln\delta$ a parameter is, however, far more efficient numerically, since self-consistency determines $\ln\delta$ directly, rather than implicitly through Eq. (3.22), which is an identity for p equal to the arbitrarily chosen μ'. Of course once we have obtained a solution, the two approaches are identical. Of course, δ can be regarded as a dynamically generated infrared cutoff. *A priori,* its value could be anything. Remarkably, we find that δ/μ is always $\sim 10^{-2}$–10^{-3}, so that δ is a few MeV—quite a sensible value.

We choose a parametrization for $\mathcal{F}_R(p)$ which not only vanishes at small p^2, but also reproduces the asymptotic form Eq. (3.18). We use

$$\mathcal{F}_R(p)=\sum_{n=1}^{N}\frac{f_n p^2}{p^2+r_n^2}\ , \tag{3.24}$$

where f_n, r_n are parameters to be determined.[17] The use of such a form in a numerical problem may appear to have prejudged that $\mathcal{F}_R(p)\to 0$ as $p\to 0$. However, we can equally well consider adding a constant f_0 to Eq. (3.24) and then, as discussed in Ref. 13, f_0 would be found to be $\sim 10^{-2}$, its exact value depending on the range of p^2 over which consistency with Eqs. (3.22) and (3.23) is imposed. Justified by this and in keeping with the analytic arguments given before, we report only solutions with $f_0\equiv 0$ here. Again we choose $\mu^2=10$ GeV^2 and set $\mathcal{F}_R(\mu)=1$. Remarkably we find adequate input-output agreement to within 1% for $N=1$, a result of the simple asymptotics for $\mathcal{F}$ in the Landau gauge. Other gauges[13,10] would require more complicated forms. We solve Eq. (3.23) for a range of values of $\alpha_s(\mu)$ as before. The results are plotted in Fig. 6 and the parameters for the $\alpha_2(\mu)=0.25$ case listed in Table II.

We have been able to show numerically, that the fermion equation does indeed have a solution vanishing as $p^2\to 0$, as found in an axial gauge by Ball and Zachariasen.[7] This behavior is the direct result of the infrared enhancement of the gluon propagator. This means, as seen from Fig. 6, that though massless quarks do propagate as essentially free particles over short distances (large momenta), over long distances (small momenta) their propagation is suppressed. Here large and small are relative to a scale Λ related to the usual scale of QCD. Indeed this suppression is sufficient to remove the particle pole on mass shell at $p^2=0$. This surely is an aspect of a confining theory. More detailed discussion of all our results appears in Sec. V.

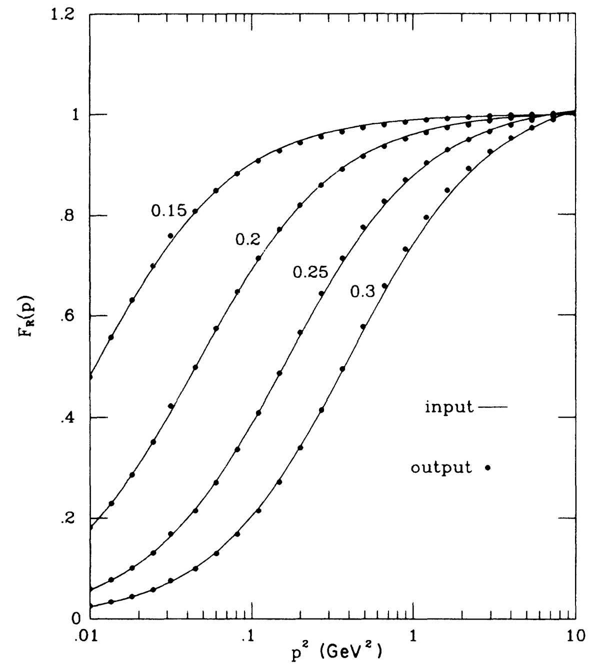

FIG. 6. Fermion renormalization function $\mathcal{F}_R(p)$ as a function of p^2 for four values of $\alpha_1(\mu)=0.15$, 0.2, 0.25, 0.3 determined from the gluon function $\mathcal{G}_R(p)$ with $n_f=0$ of Fig. 4.

IV. QUARK LOOPS

Our solutions obtained so far should be self-consistent, as long as the dynamical effect of fermion loops in the gluon equation are small. Preliminary studies[10] indicate that this is not so, and we therefore must return to the gluon equation, this time including the contribution of quark loops, shown diagrammatically in Fig. 2(b). The contribution of one massless fermion is given by

$$\Pi_F^{\mu\nu}=\Pi_F(\delta^{\mu\nu}p^2-p^\mu p^\nu)$$
$$=-\frac{g_0^2T_F}{16\pi^4}\int d^4k\frac{\mathrm{Tr}[\gamma^\mu S_F(k)\Gamma_L^\nu(k,k')S_F(k')]}{k^2k'^2}\ . \tag{4.1}$$

TABLE II. Parameters of the quark function $\mathcal{F}_R(p)$ as specified in Eq. (3.24) for the solution with $\alpha_2(\mu)=0.25$ for $n_f=0,2,4,6$.

n_f	0	2	4	6
f_1	1.0208	1.0095	1.0086	0.9972
r_1 (GeV)	0.4049	0.2980	0.1998	0.1167
δ (MeV)	8.905	12.444	12.394	10.268

Here Π_F is the fermion loop contribution to the gluon self-energy, T_F is the appropriate color trace, with the other quantities defined in Sec. III. Using our form for the longitudinal part of the quark-gluon vertex, Eq. (3.5), and our explicit parametrization of the fermion renormalization function $\mathcal{F}_R(p)$, all the integrations in Eq. (4.1) can be performed analytically. With $\mathcal{F}_R(p)$ simply represented by $f_1 p^2/(p^2+r_1^2)$, we find

$$\Pi_F = \frac{f_1 g_0^2 T_F}{12\pi^2 p^2}\left[\frac{3}{2}\frac{(p^2+r_1^2)^2}{p^2}\ln\left[\frac{p^2+r_1^2}{r_1^2}\right] - \frac{5}{6}p^2 + \frac{5}{2}r_1^2 - (4r_1^2 p^2 + p^4)^{1/2}\left[\frac{r_1^2}{p^2}+\frac{1}{4}\right]\ln\left[\frac{(p^2+r_1^2)(4r_1^2+p^2)^{1/2}+(p^2)^{1/2}(3r_1^2+p^2)}{[(4r_1^2+p^2)^{1/2}-(p^2)^{1/2}]r_1^2}\right]\right] - \frac{f_1 g_0^2 T_F}{12\pi^2}\ln\left[\frac{\kappa^2}{r_1^2}\right], \tag{4.2}$$

where for the moment we have introduced an ultraviolet cutoff κ. The ultraviolet renormalization of this term (see Sec. II) essentially consists of subtracting its value at $p^2=\mu^2$. From Eq. (4.2) we write

$$\Pi_F = \frac{f_1 g_0^2 T_F}{12\pi^2}\left[Q(p^2,r_1^2) - \ln\left[\frac{\kappa^2}{r_1^2}\right]\right] \tag{4.3}$$

giving us the renormalized contribution of the fermion loops to the inverse gluon propagator

$$\Pi_F^R = \frac{f_1 \alpha_3(\mu) T_F}{3\pi}[Q(p^2,r_1^2) - Q(\mu^2,r_1^2)] , \tag{4.4}$$

where the coupling $\alpha_3(\mu)$ is defined from $g^2(\mu) = Z_G(\kappa/\mu)Z_F(\kappa/\mu)g_0^2/Z_{\rm IR}(\lambda/\mu)$, where Z_G, Z_F are given by Eqs. (2.4) and (3.13). It can be explicitly checked that $Q(p^2,r_1^2)$ is well behaved in the limits $p^2\to 0$, $r_1^2 \to 0$ as it should be. Note that in Eq. (4.2) we have reproduced the correct perturbation logarithmic divergence.

Our next step is to include n_f flavors of massless fermions in the gluon equation, Eq. (2.7) by adding Eqs. (4.1) and (4.4) to Eqs. (2.2) and (2.3) and solving the resulting equation, together with the fermion equation, Eq. (3.23), as a coupled system. The two equations involve the two unknown functions $\mathcal{G}_R(p)$, $\mathcal{F}_R(p)$ with all other quantities specified. To deal with both equations simultaneously, however, is a cumbersome numerical exercise, so we adopt an iterative approach. In the limit $n_f=0$ the solutions obtained in Secs. II and III satisfy the coupled system identically. For nonzero n_f we take our solution for $\mathcal{F}_R(p)$ and include it in the fermion loops in the gluon equation. This is then solved to give a new $\mathcal{G}_R(p)$, which in turn is substituted into the fermion equation. This too is resolved. This is repeated until we have found self-consistent solutions to both equations. It is found that this procedure converges relatively quickly so long as n_f, the number of flavors is varied in small steps. Self-consistent solutions for both $\mathcal{G}_R(p)$ and $\mathcal{F}_R(p)$ are obtained for $n_f=0$ to $n_f=6$. The results for $n_f=0,2,4,6$ are plotted in Figs. 7 and 8 and the parameters of the $\alpha(\mu)=0.25$ solutions given in Tables I and II.

V. DISCUSSION

The truncation of the Schwinger-Dyson equations, which is necessary to make the study of the two-point functions tractable, means that we have not treated the three-point and higher functions precisely. Thus the renormalized couplings we have introduced $\alpha_i(\mu)$ $(i=1,2,3)$ are not equivalent as gauge invariance demands. Each of these can be expressed perturbatively as

$$\frac{1}{\alpha_i(p)} = \frac{1}{\alpha_i(\mu)} + \frac{\beta_0^{(i)}}{4\pi}\ln\frac{p^2}{\mu^2} = \frac{\beta_0^{(i)}}{4\pi}\ln\frac{p^2}{\Lambda_i^2} \tag{5.1}$$

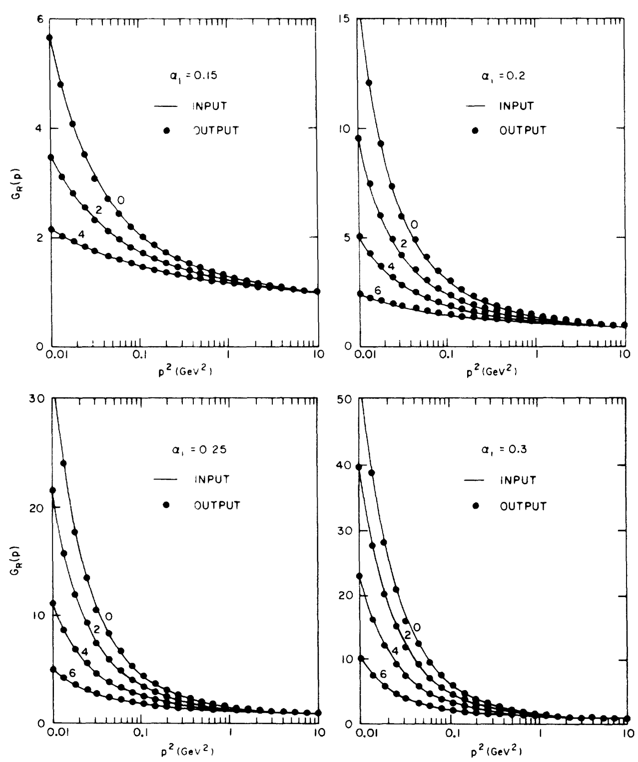

FIG. 7. Gluon renormalization function $\mathcal{G}_R(p)$ as a function of p^2 for $n_f=0,2,4,6$ and (a) $\alpha_1(\mu)=0.15$, (b) $\alpha_1(\mu)=0.2$, (c) $\alpha_1(\mu)=0.25$, and (d) $\alpha_1(\mu)=0.3$.

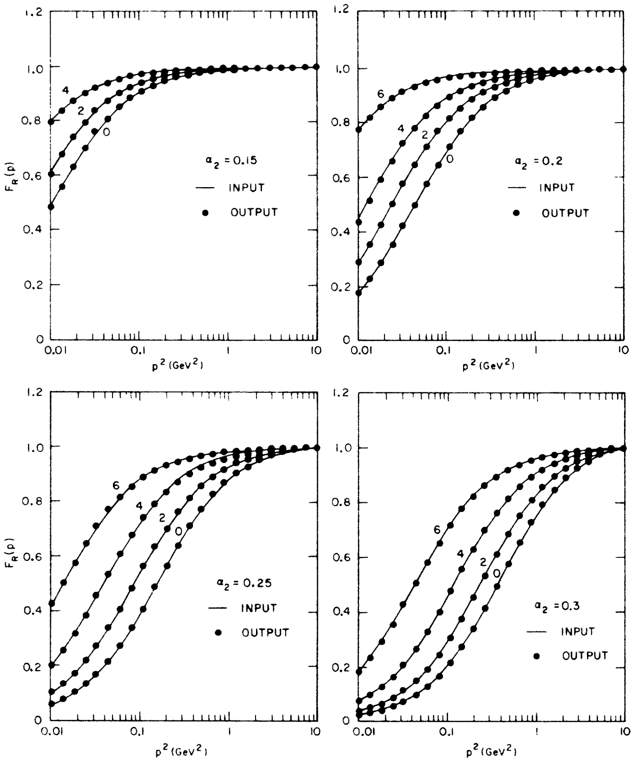

FIG. 8. Fermion renormalization function $\mathcal{F}_R(p)$ as a function of p^2 for $n_f=0,2,4,6$ and (a) $\alpha_1(\mu)=0.15$, (b) $\alpha_1(\mu)=0.2$, (c) $\alpha_1(\mu)=0.25$, and (d) $\alpha_1(\mu)=0.3$.

which specifies $\beta_0^{(i)}$ and the scale parameter Λ_i. A complete analysis would make all of these equal. However, our treatment is inevitably imperfect for the three-point functions. This is reflected here in the differences

$$\begin{aligned}
\beta_0' &= 2\gamma_0 = 2(\tfrac{7}{3}C_A - \tfrac{4}{3}n_f T_F)\ ,\\
\beta_0'' &= \tfrac{7}{3}C_A + \tfrac{3}{4}C_F\ ,\\
\beta_0''' &= \tfrac{7}{3}C_A\ .
\end{aligned} \tag{5.2}$$

Of course, the exact lowest-order perturbative results $\beta_0=\frac{11}{3}C_A-\frac{4}{3}n_F T_F$ and (in the Landau gauge) $\gamma_0=\frac{13}{6}C_A-\frac{4}{3}n_F T_F$ are both independent of the Casimir C_F as a result of gauge invariance.

Our equations, Eqs. (2.7) and (3.23), depend explicitly only on $\alpha_i(\mu)$, which we have taken to be equal. Although, of course, the running of the coupling does implicitly enter in the equations for $\mathcal{G}_R(p)$, $\mathcal{F}_R(p)$. Nevertheless, at a practical level, our renormalizations have made the equations ultraviolet finite independently of any particular parametrization of the functions $\mathcal{F}_R(p)$, $\mathcal{G}_R(p)$. In this sense, the forms of the renormalization are forced upon us and provide a convenient modeling of the effect of the ultraviolet renormalizations.

Using these prescriptions we have studied the gluon and quark propagators in QCD at essentially all relevant momenta using the Schwinger-Dyson equations. The beauty of this approach is that with a suitable truncation these equations allow such quantities to be studied to all orders in perturbation theory. The first step in this program is the investigation of the gluon propagator in the pure gauge sector. As reviewed in Sec. II, this behaves effectively like $1/p^4$ for small momenta and perturbatively as a logarithm of p^2 at large momenta. These are features of all our solutions for all values of the coupling $\alpha_1(\mu)$ we have considered. It is clear from Fig. 4 that the small and large momenta regimes are delineated by Λ_1. Indeed, the coefficient of the enhanced term, viz., $A\mu^2$, Eq. (2.12), is well represented by a form of Λ_1^2 times $\ln\mu^2/\Lambda_1^2$ to a power (see Fig. 9). The appearance of the logarithms we believe to be a reflection of the fact that the exact form for $G(p)$ is really $1/p^2$ modified by logarithms, which we have neglected in the simple expression, Eq. (2.12), and so are mocked up by the constant A.

The infrared enhancement of the gluon propagator we find implies a Wilson area law,[18] which many regard as a criterion for confinement. At a more naive level, the Fourier transform of the time-time component of the full

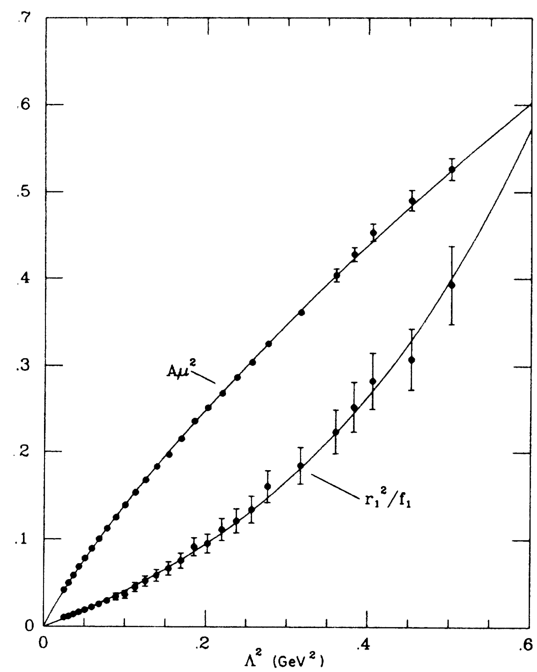

FIG. 9. Scales of the gluon's infrared enhancement, $A\mu^2$ from Eq. (2.12), and of the quark's suppression, r_1^2/f_1 from Eq. (3.24), marked by dots as functions of Λ_1^2, Eqs. (5.1) and (5.2) for our $n_f=0$ solutions. The error bars were determined from an analysis of the input/output agreement of these solutions. The curves show

$$A\mu^2 = 0.497\Lambda_1^2\left[\ln\frac{\mu^2}{\Lambda_1^2}\right]^{0.673}\ ,$$

$$\frac{r_1^2}{f_1} = \Lambda_1^2\left[0.36+107\left[\ln\frac{\mu^2}{\Lambda_1^2}\right]^{-5}\right]\ .$$

These are more to guide the eye than serious analytic expressions.

gluon propagator is related to the potential between static color charges. For completeness we show the potential so derived from our $\alpha(\mu)=0.25$ solution in Fig. 10. The infrared enhancement generates a linear increase in this potential at large distances. This is, of course, only the one-gluon-exchange contribution to the potential, which is necessarily vector in character. The complete potential (in a non-Abelian theory) is not a simple iteration of the one-boson-exchange term, but involves multigluon exchanges, too.[20] These inevitably generate a scalar component to this potential and it would be interesting to know how this compared with the simple vector part we can readily compute, which on its own would lead to a Klein paradox. However, the calculation of the complete potential involves an understanding of the full four-fermion Green's function, which we are far from being able to treat.

We now turn to the fermion equation, Eq. (3.23). As mentioned at the end of Sec. III we have shown that a consistent solution exists for massless quarks, which has a vanishing propagator at small p^2. This can be seen as the nonpropagation of quarks over large distances. Again the momentum scale at which this suppression arises is related to Λ of Eqs. (5.1) and (5.2). Just as the enhancement of the gluon is parametrized by $A\mu^2/p^2$, the suppression of the quark is represented by $f_1 p^2/r_1^2$ and just as $A\mu^2 \sim \Lambda_1^2$ modulated by logarithms, $(r_1^2/f_1) \sim \Lambda_1^2$ modified by logarithms, too. This is borne out by Fig. 9.

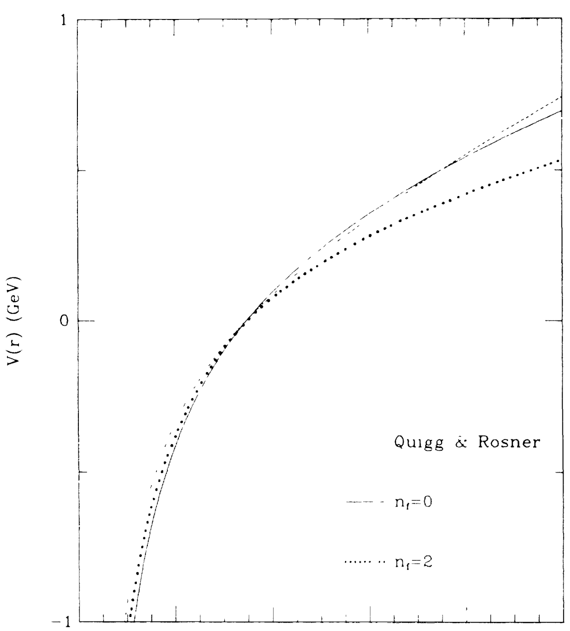

FIG. 10. One-gluon-exchange contribution to the static interquark potential $V(r)$ as a function of r from our solution for the gluon propagator for $\alpha_1(\mu)=0.25$ with $n_f=0$ (solid line) and $n_f=2$ (dotted line). The renormalization constant has been chosen (somewhat arbitrarily) to maximize agreement with the phenomenological potential of Quigg and Rosner (Ref. 19) in the region determined by the $c\bar{c}$ and $b\bar{b}$ spectra. Their potential is shown for comparison.

In contrast, the other dimensional parameter δ, introduced in Sec. III, has no obvious Λ dependence being always around 10 MeV. As a dynamically generated infrared cutoff this is a physically sensible value and perhaps bodes well for the study of fermion solutions that break chiral symmetry, to which we shall return in Ref. 16.

The contribution that quark loops make to the gluon propagator is found to be sizable (as in Ref. 10) and so, in Sec. IV, we have solved the gluon and quark equations simultaneously. Although the gluon propagator remains enhanced at low momentum and the quark propagator suppressed there, too, a nonzero n_f significantly dampens both effects. The gluon is no longer so strongly enhanced and though for more flavors the intrinsic scale Λ_1, Eqs. (5.1) and (5.2), decreases, just as it does in perturbation theory, the coefficient of the pole decreases more dramatically. For $\alpha_1(\mu)=0.3$, the introduction of two flavors of fermion reduces the enhanced term to 70% of its $n_f=0$ value. For four flavors, this figure is 40%. The effect is more pronounced for smaller α_1, being 45% and 18%, respectively, for $\alpha_1(\mu)=0.15$. Thus with more than eight flavors of massless quarks, we suspect no enhancement will occur. This trend is seen in the parameters of Table I. Consequently, the Fourier transform of the gluon propagator now has a smaller increase at large distances, as shown in Fig. 10 for $n_f=2$. Although this is only for the single-gluon-exchange part of the potential, it does indicate that with a number of massless fermions much greater than three, deconfinement will occur. Although perturbatively virtual $q\bar{q}$ pairs do screen the color charge, here in the nonperturbative regime of low momenta, their effect is far greater than the naive counting of N_c: $\frac{2}{11}n_f$ of Eq. (3.1) would suggest.

Although the solutions of Figs. 7 and 8 are for "real" QCD with $N_c=3$, they can equally well describe the solutions for any $N_c \geq 3$ where $\alpha_s \to 3\alpha_s/N_c$ and $n_f \to n_f N_c/3$. Thus, for example, Fig. 7(d) with $\alpha(\mu)=0.3$ and $N_c=3$ and $n_f=0,2,4,6$ can be regarded as a plot with $\alpha(\mu)=0.15$, $N_c=6$, and $n_f=0,4,8,12$, respectively. So, as expected, for large N_c, a fixed number of flavors play a smaller role in keeping with the philosophy of the $1/N_c$ expansion. However, $N_C=3$ is very far from the large-N limit as far as fermion flavors are concerned. A heuristic criterion for neglecting the fermion contributions in the low-momentum region would appear to be simply $n_f/N_c < 1$, whereas at high-momentum only $2n_f/11N_c \ll 1$ is required. Thus in the real world with $N_c=3$, fermions play a crucial role in strong-interaction physics.

Although the quantitative aspects of our analysis surely depend on our particular simplification of the Schwinger-Dyson equations needed to make the problem tractable, the resulting behavior of the quark and gluon propagators is nevertheless consistent with their being free over short distances yet completely confined inside hadrons as experiment requires. These qualitative successes validate the use of the Schwinger-Dyson equations as a means of calculating effects beyond the reach of perturbation theory.

ACKNOWLEDGMENTS

N.B. would like to thank the Science and Engineering Research Council, United Kingdom, for financial support and W. J. Marciano and the theory group at BNL for their kind hospitality. M. R. P. acknowledges the receipt of a Fulbright travel grant. This manuscript has been authored under Contract No. DE-AC02-76CH00016 with the U.S. Department of Energy.

[1]For a review, see B. R. Webber, Annu. Rev. Nucl. Part. Sci. **36**, 253 (1986).

[2]R. L. Stuller, Phys. Rev. D **13**, 513 (1976); H. Pagels, *ibid.* **14**, 2747 (1976); **15**, 2991 (1977).

[3]J. S. Ball and F. Zachariasen, Nucl. Phys. **B143**, 148 (1978); C. Nash and R. L. Stuller, Proc. R. Irish Acad. **78**, 217 (1978); R. Anishetty, M. Baker, S. K. Kim, J. S. Ball, and F. Zachariasen, Phys. Lett. **86B**, 52 (1979); M. Baker, J. S. Ball, P. Lucht, and F. Zachariasen, *ibid.* **89B**, 211 (1980).

[4]M. Baker, J. S. Ball, and F. Zachariasen, Nucl. Phys. **B186**, 531 (1981); **B186**, 560 (1981).

[5]S. Mandelstam, Phys. Rev. D **20**, 3223 (1979).

[6]U. Bar-Gadda, Nucl. Phys. **B163**, 312 (1980); A. I. Alekseev, Yad. Fiz. **33**, 516 (1981) [Sov. J. Nucl. Phys. **33**, 269 (1981)]; W. J. Schoenmaker, Nucl. Phys. **B194**, 535 (1982); B. A. Arbuzov, Phys. Lett. **125B**, 497 (1983); E. J. Gardner, J. Phys. G **9**, 139 (1983); D. Atkinson, P. W. Johnson, W. J. Schoenmaker, and H. A. Slim, Nuovo Cimento **A77**, 197 (1983); J. L. Rodriquez Marrero and A. R. Swift, Phys. Rev. D **29**, 1823 (1984); **31**, 917 (1985); **32**, 476 (1985).

[7]J. S. Ball and F. Zachariasen, Phys. Lett. **106B**, 133 (1981).

[8]N. Brown and M. R. Pennington, Phys. Lett. B **202**, 257 (1988); **205**, 596(E) (1988).

[9]N. Brown, Ph.D. thesis, University of Durham, 1988 (unpublished); N. Brown and M. R. Pennington (in preparation).

[10]M. R. Pennington, Phys. Rev. Lett. **60**, 267 (1988).

[11]J. S. Ball and T. W. Chiu, Phys. Rev. D **22**, 2550 (1980).

[12]S. K. Kim and M. Baker, Nucl. Phys. **B164**, 152 (1980).

[13]A. D. Worrall, Ph.D. thesis, University of Durham, 1985 (unpublished); M. R. Pennington and A. D. Worrall (unpublished).

[14]T. Maskawa and H. Nakajima, Prog. Theor. Phys. **52**, 1326 (1974); **54**, 860 (1975); K. Higashijima, Phys. Rev. D **29**, 1228 (1984); R. Pisarski, *ibid.* **29**, 2423 (1984); V. A. Miranskii and P. I. Fomin, Fiz. Elem. Chastits. At. Yad. **16**, 469 (1985) [Sov. J. Part. Nucl. Phys. **16**, 203 (1985)]; R. Casalbuoni, S. de Curtis, D. Dominici, and R. Gatto, Phys. Lett. **150B**, 295 (1985); B. Holdom, *ibid.* **150B**, 301 (1985); T. W. Appelquist, M. Bowick, D. Karabali, and L. C. R. Wijewardhana, Phys. Rev. D **33**, 3704 (1986); D. Atkinson and P. W. Johnson, J. Math. Phys. **28**, 2488 (1987); D. Atkinson, P. W. Johnson and M. Koopmans, Z. Phys. C **34**, 99 (1987); D. Atkinson, P. W. Johnson, and K. Stam, Phys. Lett. B **201**, 105 (1988).

[15]J. M. Cornwall, Phys. Rev. D **22**, 1452 (1980); V. S. Gogokhia and B. A. Magradze, Central Research Institute for Physics, Budapest, Report No. KFKI-1987-01/A, 1987 (unpublished).

[16]N. Brown and M. R. Pennington (work in progress).

[17]See the discussion in Sec. II on parametrizations.

[18]G. B. West, Phys. Lett. **115B**, 468 (1982).

[19]C. Quigg and J. L. Rosner, Phys. Rep. **56**, 167 (1980).

[20]T. Appelquist, M. Dine, and I. J. Muzinich, Phys. Lett. **69B**, 231 (1977); F. Feinberg, Phys. Rev. Lett. **39**, 316 (1977); W. Fischler, Nucl. Phys. **B129**, 157 (1977).